

Protonic Conduction Properties of Nanostructured Gd-doped CeO₂ at Low Temperatures

Hee Jung Park[†], Jae Soo Shin, Yong Ho Choa*, Han Bok Song*,
Ki Moon Lee**, and Kyu Hyoung Lee***[‡]

Dep. of Advanced Materials Engineering, Daejeon University, Daejeon 34520, Korea

**Dep. of Chemical Engineering, Hanyang University, Ansan 04763, Korea*

***Dep. of Physics, Kunsan Nat. University, Kunsan 54150, Korea*

****Dep. of Nano Applied Engineering, Kangwon Nat. University, Chuncheon 24341, Korea*

(Received August 28, 2015; Revised September 21, 2015; Accepted September 21, 2015)

ABSTRACT

The electrical properties of nanostructured Gd-doped CeO₂ (n-GDC) as a function of temperature and water partial-pressure were investigated using ac and dc measurements. For n-GDC, protonic conductivity prevails under wet condition and at low temperatures (< 200°C), while oxygen ionic conductivity occurs at high temperatures (> 200°C) under both dry and wet conditions. The grain boundaries in n-GDC were highly selective, being conductive for protonic transport but resistive for oxygen ionic transport. The protonic conductivity reaches about 4×10^{-7} S/cm at room temperature (RT).

Key words : Nanostructure, Protonic conductor, Ceria

1. Introduction

Ceramics used in the electrolytes of fuel cells are commonly polycrystalline forms made up of grains and grain boundaries (gb). The crystal periodicity of the grains in the grain boundary can be disrupted by strain, dangling bonds, and open structures, so that the crystal structure of the gb differs from that of the grain. This disruption leads to changes in the concentrations and mobility of the protonic charge carriers, and thus their conductivity in the gb can be different from that of the grain.^{1,2)} In most cases, it has been reported that the gb conductivity is a few of orders of magnitude lower than that of the grain because of the irregularity and distortion of the gb.²⁻⁵⁾ For instance, in doped-BaZrO₃, which is a well-known perovskite with high protonic conductivity, the overall protonic conductivity is below 10⁻⁶ S/cm at 300 °C even though the protonic conductivity in the grain is 10⁻²⁻³ S/cm at that temperature.^{2,6)} So, not that long ago, it was generally believed that the gb was not a preferable pathway for protonic conduction in dense ceramics. However, in very recent years, some results that have broken this common assumption have been reported in nanostructured ceramics.⁷⁻¹⁰⁾

Guo et al.⁷⁾ first attempted to determine whether water affected conduction by making a nanostructure with yttria stabilized zirconia (YSZ) film; they reported that protonic defects were found to form on the surface and diffuse along the gb into the interior of the specimen in boiling water. Anselmi-Tamburini et al.⁸⁾ also measured protonic conduction in highly dense nanostructured YSZ with a grain size of ~ 15 nm. Kim et al.⁹⁾ confirmed this result by first making a new type of fuel cell operating at room temperature. After Kim's study, a number of studies investigating the protonic conductivities and the conduction mechanisms of nanocrystalline materials followed.¹⁰⁻¹³⁾ S. Miyoshi et al.,¹⁰⁾ M. Shirpour et al.¹¹⁾ and C. Tande et al.¹²⁾ showed again that the gb in dense nanostructured zirconia and ceria are highly selective for protonic transport, proving the protonic gb conduction. However, in spite of this interesting finding in the field of nanocrystalline, some tasks that need to be studied still remain with respect to applications. The first is that the reported protonic conductivity is low (the protonic conductivity of nanocrystalline zirconia is ~ 10⁻⁹ S/cm at RT); the second is that little has been done for the conduction properties of nanostructured ceria, while a number of studies on the protonic conductivity and conduction mechanism of nanostructured zirconia have been performed. So, herein, we have tried to study the protonic conduction properties of nanostructured 10 mol% Gd-doped CeO₂ (n-GDC) as a function of temperature and water partial pressure with ac measurements.

[†]Corresponding author : Hee Jung Park

E-mail : hjpark@dju.kr

Tel : +82-42-280-2417 Fax : +82-42-280-2418

[‡]Corresponding author : Kyu Hyoung Lee

E-mail : khlee2014@kangwon.ac.kr

Tel : +82-42-280-2417 Fax : +82-42-280-2418

2. Experimental Procedure

Commercial GDC (10% Gd-doped CeO₂, FCM) nano-powders were used (the size of the powders is 5 ~ 10 nm). For the preparation of highly dense nanocrystalline material, the Spark Plasma Sintering (SPS) technique was used for very limited grain growth during sintering. The nanopowders were poured into a mold and sintered using a SPS (Syntex) at 750 °C and 600 MPa for 5 min. In order to apply high pressure to the mold, a double acting die consisting of graphite molds (outer and inner), silicon carbide punches, and tungsten carbide spacers was used (all of the components were purchased from Komexcarbon).¹⁴⁾ The sintered sample was very dense (> 95%) and the average grain size of the sample was ~ 35 nm.¹⁵⁾ For comparison, microstructured GDC (m-GDC) with an average grain size of ~ 3 mm was prepared. In order to obtain a microcrystalline, a conventional ceramic process was carried out (the detailed description is reported elsewhere).¹⁶⁾

For electrical measurements, the surface of the sintered pellet was polished using SiC-paper; then, Pt-paste was painted onto both surfaces. The electrical resistance of the pellet was measured as a function of temperature by using 2-probe ac impedance spectroscopy (Impedance analyzer: Material Mates 7260) and dc measurement (Keithley 2400 source-measure unit) in dry and wet air (water partial pressure, $P_{\text{H}_2\text{O}} \sim 2.3 \times 10^{-2}$ atm). The electrical resistance was also examined as a function of $P_{\text{H}_2\text{O}}$.

EMF (open circuit electromotive force) was checked using a concentration cell consisting of n-GDC, Pt-pastes, and an alumina-tube as solid electrolyte, electrodes, and support, respectively (see Ref. 9). EMF was measured as a function of $P_{\text{H}_2\text{O}}$ of one side of the cell while exposing the other side of the cell to pure water.

3. Results and Discussion

Figure 1 shows the representative impedance spectra of n-GDC, measured at (a) 250°C and (b) 100°C under dry and

wet air. Both spectra, obtained at high temperature (250°C), consist of a large semicircular arc partially overlapped with another arc that appears at higher frequencies. It should be noted that there is a small arc at high frequencies, even though it is difficult to distinguish the arcs clearly with the unaided eye (sample can be seen more clearly in the inset). The two semicircular arcs are associated with the grain (high frequency region) and gb (middle and low frequency regions) impedance. As can be seen, the arc corresponding to the grain is so small, compared with that of the gb, that it can be ignored. Accordingly, the gb dominates the overall conductance in n-GDC at the given temperature. Fig. 1(a) also shows that the shape and size of the impedance patterns obtained under dry (black symbol) and wet air (blue symbol) are similar. This means that the sample resistances are almost unchanged with the change of $P_{\text{H}_2\text{O}}$, showing that the charge carriers are independent of $P_{\text{H}_2\text{O}}$. It is well known that doped-ceria is a good oxygen ionic conductor. So, at the high temperature, the charge carriers are surely oxygen ions rather than protonic defects.

Unlike the spectra at high temperature, the spectra of n-GDC at low temperature (100°C) under the wet condition consist of a singular semicircular arc; spectra size is much smaller than that of the spectrum under dry condition (Fig. 1(b)). This means that the sample under wet air becomes conductive as a result of the charge carriers generated from the water vapor. The charge carriers are protonic defects (this will be discussed later).

Figure 2 shows the Arrhenius plot of the conductivity of n-GDC under dry and wet air. For comparison, the conductivity of m-GDC was also investigated as a function of temperature, and the two results are plotted together in Fig. 2. The conductivity (s) was computed using the relation $s = (1/R)(d/A)$, with R being the total resistance; d and A are the sample distance and the area, respectively. As can be seen in n-GDC, s_{dry} (the conductivity under dry air) shows linear behavior with the activation energy (E_a) ~ 0.90 eV, which is consistent with the reported value, showing that the charge carriers are oxygen ions (it should be noted that doped ceria

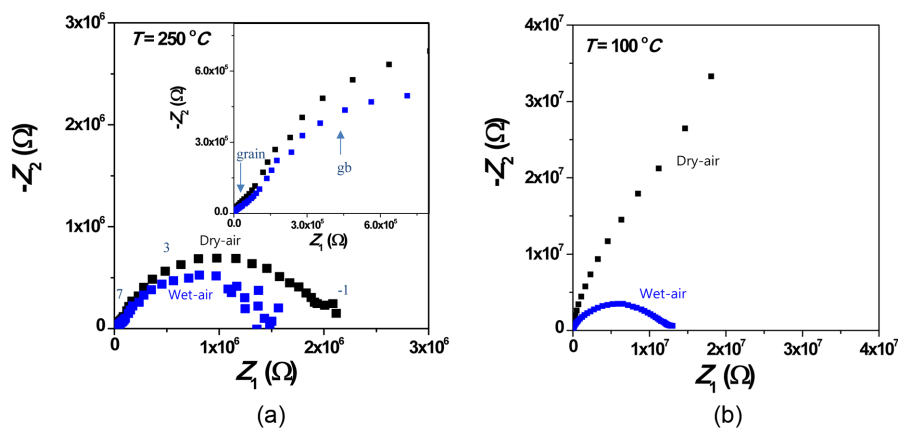


Fig. 1. Impedance spectra of n-GDC under dry and wet air at (a) 250°C and (b) 100°C, respectively. The inset shows the spectra in the high frequency region. Numbers indicate measured frequencies on a logarithmic scale.

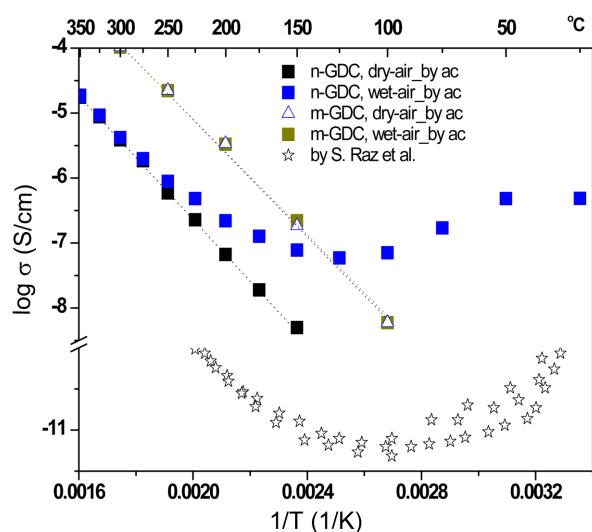


Fig. 2. Arrhenius plots of the conductivities of n-GDC (nanostructured ceria) and m-GDC (microstructured ceria) under dry and wet air. The reported protonic conductivity of porous zirconia is provided for comparison.¹⁸⁾

is a very well-known oxygen ionic conductor, so it is being used as a solid electrolyte of SOFCs).¹⁷⁾

On the other hand, s_{wet} (the conductivity under wet-air) begins to deviate from s_{dry} at around 225°C, increasing with the decrease of the temperature down to RT . This upturn of s_{wet} is due to the hydration of n-GDC, which gives rise to a crossover from oxygen-ions to protons. As discussed above, these protonic charge carriers, appearing under wet air and at low temperatures, go through the nanocrystalline along the gb. s_{wet} was $\sim 4 \times 10^{-7}$ S/cm at RT (it should be noted that s_{wet} of nanostructured zirconia was reported to be $\sim 10^{-9}$ S/cm).¹³⁾

In order to prove that the protons conduct along the gb, the conductivity of m-GDC was measured. Unlike n-GDC, m-GDC has conductivity under wet air that does not show upturn behavior (the conductivity decreases linearly with decreasing temperature). This is surely due to the low density of the gb within m-GDC. The grain sizes of n-GDC and m-GDC are ~ 30 nm and ~ 3 mm, respectively, so the gb density in m-GDC is at least several orders of magnitude lower than that in n-GDC.

Another piece of evidence for protonic conduction along the gb is seen in the EMF-results of the concentration cell (EMF test configuration is shown in Fig. 3). As can be seen in Fig. 3, EMFs were observed as a function of $P_{\text{H}_2\text{O}}$ of one side of the cell because different chemical potential gradients between the inside and outside of the cell make different EMFs, indicating the protonic conduction within n-GDC. Even though the short circuit currents of the cell are not shown here, they were also observed in the cell constructed with n-GDC (it should be noted that the short-circuit currents in the cell constructed with m-GDC could not be clearly observed). Besides the conductivity tests of n-

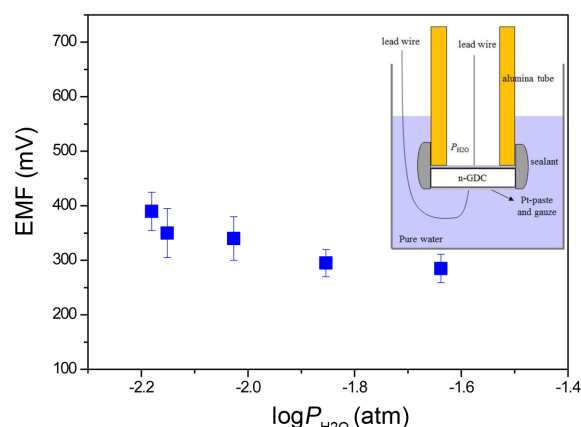


Fig. 3. EMF values measured in the water concentration cell at room temperature. One side of the cell was immersed in pure water while exposing the other side of the cell to wet air.

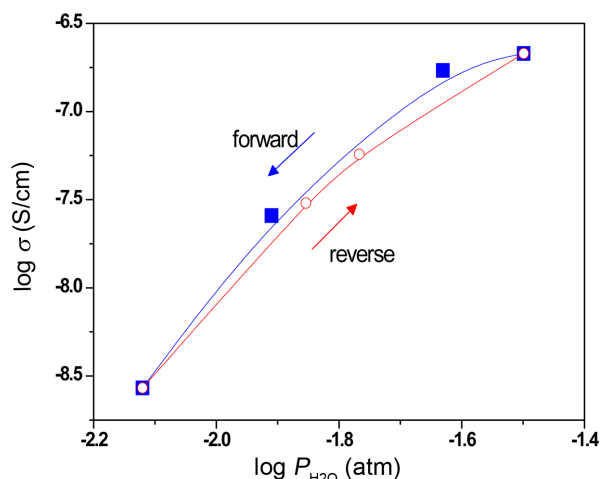


Fig. 4. The dependence of $P_{\text{H}_2\text{O}}$ in n-GDC is exhibited at 80°C.

GDC and m-GDC, based on the cell test, the fact that the protonic charge carriers go through the gb is clear.

Be that as it may, the exact conduction mechanism of the protonic charge carriers in the gb has still not been revealed. S. Raz et al.¹⁸⁾ investigated the protonic conduction behavior of porous zirconia (data is inserted in Fig. 2). They found that the proton transport originates with physisorption and chemisorption reactions on the zirconia surfaces. They insisted that the physisorption reaction takes place dominantly at low temperatures ($< 100^\circ\text{C}$), while the chemisorption reaction occurs at high temperatures ($> 100^\circ\text{C}$). As can be seen in Fig. 2, the conduction behaviors between n-GDC and porous zirconia are very similar. Somehow, the protons in n-GDC may transfer through an open space (a free volume) of the gb by physisorption and chemisorption reactions like the mechanism suggested by S. Raz et al.¹⁸⁾ (it should be noted that the gb also has dangling bonds and free volumes).

Figure 4 shows the dependence of $P_{\text{H}_2\text{O}}$ in n-GDC at 80°C.

The solid and open symbols represent the forward direction ($P_{\text{H}_2\text{O}}$ changes high to low) and reverse direction ($P_{\text{H}_2\text{O}}$ changes low to high), respectively. As can be seen, the protonic conductivity decreases with decreasing $P_{\text{H}_2\text{O}}$ (forward direction) and comes back (reverse direction) with increasing $P_{\text{H}_2\text{O}}$ at the fixed temperature, showing that the hydration and the dehydration are nearly reversible in n-GDC.

4. Conclusions

It was observed that nanostructured Gd-doped CeO_2 has protonic conductivity under wet condition and at low temperatures. The protonic conductivity of this material reaches about 4×10^{-7} S/cm at room temperature (RT) and 23,000 ppm water pressure. The grain boundaries in the nanocrystalline were highly selective, being conductive for proton transport but resistive for oxygen ionic transport. The hydration and the dehydration processes were nearly reversible.

REFERENCES

1. R. Hino, K. Haga, H. Aita, and K. Sekita, "R&D on Hydrogen Production by High-Temperature Electrolysis of Steam," *Nucl. Eng. Des.*, **233** [1-3] 363-75 (2004).
2. K. Kreuer, "Proton-Conducting Oxides," *Annu. Rev. Mater. Res.*, **33** 333-59 (2003).
3. F. Iguchi, N. Sata, T. Tsurui, and H. Yugami, "Microstructures and Grain Boundary Conductivity of $\text{BaZr}_{1-x}\text{Y}_x\text{O}_3$ ($x = 0.05, 0.10, 0.15$) Ceramics," *Solid State Ionics*, **178** [7-10] 691-95 (2007).
4. H. Bohn and T. Schober, "Electrical Conductivity of the High-Temperature Proton Conductor $\text{BaZr}_{0.9}\text{Y}_{0.1}\text{O}_{2.95}$," *J. Am. Ceram. Soc.*, **83** [4] 768-72 (2000).
5. R. Slade, S. Flint, and N. Singh, "Investigation of Protonic Conduction in Yb- and Y-Doped Barium Zirconates," *Solid State Ionics*, **82** [3-4] 135-41 (1995).
6. R. Cervera, Y. Oyama, S. Miyoshi, K. Kobayashi, T. Yagi, and S. Yamaguchi, "Structural Study and Proton Transport of Bulk Nanograined Y-doped BaZrO_3 Oxide Protonics Materials," *Solid State Ionics*, **179** [7-8] 236-42 (2008).
7. X. Guo, "On the Degradation of Zirconia Ceramics during Low-Temperature Annealing in Water or Water Vapor," *J. Phys. Chem. Solids*, **60** [4] 539-46 (1999).
8. U. Anselmi-Tamburini, F. Maglia, G. Chiodelli, P. Riello, S. Bucella, and Z. Munir, "Enhanced Protonic Conductivity in Fully Dense Nanometric Cubic Zirconia," *Appl. Phys. Lett.*, **89** 163116-19 (2006).
9. S. Kim, U. Anselmi-Tamburini, H. Park, M. Martin, and Z. Munir, "Unprecedented Room-Temperature Electrical Power Generation using Nanoscale Fluorite-Structured Oxide Electrolytes," *Adv. Mat.*, **20** [3] 556-59 (2008).
10. S. Miyoshi, Y. Akao, N. Kuwata, J. Kawamura, Y. Oyama, T. Yagi, and S. Yamaguchi, "Low-Temperature Protonic Conduction Based on Surface Protonics: An Example of Nanostructured Ytria-Doped Zirconia," *Chem. Mater.*, **26** [18] 5194-200 (2014).
11. M. Shirpour, G. Gregori, R. Merkle, and J. Maier, "On the Proton Conductivity in Pure and Gadolinium Doped Nanocrystalline Cerium Oxide," *Phys. Chem. Chem. Phys.*, **13** [3] 937-40 (2011).
12. C. Tande, D. Perez-Coll, and G. Mather, "Surface Proton Conductivity of Dense Nanocrystalline YSZ," *J. Mater. Chem.*, **22** 11208-13 (2012).
13. S. Kim, H. Avila-Paredes, S. Wang, C. Chen, R. De Souza, M. Martin, and Z. Munir, "On the Conduction Pathway for Protons in Nano-Crystalline Ytria-Stabilized Zirconia," *Phys. Chem. Chem. Phys.*, **11** [17] 3035-37 (2009).
14. Y. Anselmi-Tamburini, G. Garay, and Z. Munir, "Dense nanostructured oxides with fine crystals prepared by field activation sintering"; US Patent 013, 872 (October, 26, 2006).
15. H. Park and Y. Choa, "The Grain Boundary Conduction Property of Highly Dense and Nanostructured Yttrium-Doped Zirconia," *Electro. Sol. St. Lett.*, **13** [5] K49-52 (2010).
16. H. Park and G. Choi, "The Electrical Conductivity and Oxygen Permeation of Ceria with Alumina Addition at High Temperature," *Solid State Ionics*, **178** [33-34] 1746-55 (2008).
17. T. Zhang, J. Ma, Y. Leng, S. Chan, P. Hing, and J. Kilner, "Effect of Transition Metal Oxides on Densification and Electrical Properties of Si-Containing $\text{Ce}_{0.8}\text{Gd}_{0.2}\text{O}_2$ Ceramics," *Solid State Ionics*, **168** [1-2] 187-95 (2004).
18. S. Raz, K. Sasaki, J. Maier, and I. Riess, "Characterization of Adsorbed Water Layers on Y_2O_3 -Doped ZrO_2 ," *Solid State Ionics*, **143** [2] 181-204 (2001).